Dipole-allowed and dipole-forbidden l change in slow collisions of Na$^+$ with Na(28d) Rydberg atoms

K. B. MacAdam, R. G. Rolfes, X. Sun, J. Singh, W. L. Fuqua III, and D. B. Smith

Department of Physics and Astronomy, University of Kentucky, Lexington, Kentucky 40506

Both dipole-allowed and dipole-forbidden transitions occur in slow l-change collisions of Na$^+$ with Na(28d) Rydberg atoms, despite the validity of the dipole approximation. Measurements of the velocity dependence of the final-state distribution under single-collision conditions are reported. Effects of strong coupling were found, in partial agreement with recent coupled-channel calculations. Microwave-resonance techniques were used to identify the selective-field-ionization signatures of 28f, g, and h states.

I. INTRODUCTION

In l-change collisions of ions with Na(nd) Rydberg atoms,[1]

$$\text{Na}^+ + \text{Na}(nd) \rightarrow \text{Na}^+ + \text{Na}(n, l \geq 3) \ , \tag{1}$$

a distribution of final states nl is formed with the same principal quantum number n but varying orbital angular momentum l. The Na$^+$ is incident at velocity v_i on the Rydberg atoms in an atomic beam. Previous work in this laboratory has established that when the reduced velocity $\bar{v}$ is near one ($\bar{v}$ is defined as v_i/v_e, where $v_e = 1/n$ a.u. is the Bohr orbital velocity of the Rydberg electron), the cross section for (1) exceeds the geometric cross section πn^4 a.u. by 3 orders of magnitude.[1] Impact parameters b of order 10 to 100 times the Bohr orbital radius $a_n = n^2$ a.u. thus make dominant contributions to the cross section. For such large b the dipole approximation for the Coulomb potential of the ion is accurate. Yet in collisions at or below $\bar{v} = 1$ many levels may be significantly coupled by the perturbation, leading to transitions, *under single-collision conditions*, that are dipole forbidden; that is, for which $\Delta l > 1$. These transitions occur by strong coupling and require a theory that calculates the effect of the perturbing dipole potential to all orders.[2] It was shown earlier that the final-state distribution following 1-keV Ar$^+$ impact on Na(28d) ($\bar{v} = 0.89$) was very sensitive to *multiple collisions*,[3] in which a single Na(28d) target atom is struck in succession by two or more Ar$^+$ ions in an incident beam, leading to very high values of l. However, under conditions of weak ion bombardment the data were consistent with a restriction to small Δl. At the lowest bombarding current used, 56% of final $n = 28$ states had $l \leq 5$. Large changes of l are thus strongly unfavored at $\bar{v} = 0.89$ in a single encounter and are likely to be the result of multiple collisions in experiments where they are observed to be dominant.

Beigman and Syrkin[4] recently demonstrated by coupled-channel calculations that the final-l distribution for a Na(28d) target would be dominated by $l = 3$ (more than 90% of the final states) at $\bar{v} = 2$ but that for decreasing $\bar{v}$ an increasing amount of dipole-forbidden behavior would be encountered. For $\bar{v} < 0.6$, the final pop-

ulation of 28g would exceed 28f, and below $\bar{v} = 0.4$ 28h would exceed 28g. At $\bar{v} = 0.3$ more than 70% of the final $n = 28$ population would have $l > 5$. A study by Smith *et al.*[5] of K$^+$ + Na(nd) l change for $\bar{v}$ between 0.28 and 0.69 indicated a wide range of final l, but no quantitative analysis was reported. In our earlier examination[3] of final states at $\bar{v} = 0.89$ no attempt was made to separate $l = 3$, 4, and 5. Thus despite earlier indications that dipole-forbidden transitions might occur in slow inelastic collisions of ions with Na d states, no definitive experimental result was obtained, and the theoretical work was untested.

We have now obtained conclusive evidence of the increasingly dipole-forbidden character of the final-state distribution for slow collisions on Na(28d).[6] In the following sections, the collision experiment and a new method of determining the content of $l \geq 3$ states by field ionization will be described. Uncertainties in the m_l distributions and the resulting uncertainties in the l distributions will be discussed, and the experimental results will be compared with theory.

II. EXPERIMENTAL METHOD

Laser-excited Na(28d) was bombarded by Na$^+$ at incident energies 29–590 eV ($\bar{v} = 0.2$–0.9). Time-resolved selective field ionization (SFI) was used to analyze the distribution of final states.[7] A variable-slope linear positive high-voltage ramp[8] was applied to the upper of two horizontal parallel plates that formed a condensor of 1.30-cm spacing around the small volume of Na Rydberg atoms. Adiabatic and diabatic SFI (Ref. 9) were observed by detecting Na$^+$ in a shielded discrete-dynode electron multiplier positioned below a gridded hole in the lower plate. A transient digitizer recorded the adiabatic and diabatic SFI spectra (Fig. 1). The shape of the $n = 28$ impact-related diabatic SFI signal [$|m_l| \geq 3$, Fig. 1(f)] was recorded at several bombarding energies. To insure single-collision conditions the incident ion-beam intensity was reduced so that the depopulation of the adiabatic SFI signal [Fig. 1(c)] was approximately 8% after 2-μs exposure. At 50 eV it was verified that further reductions of intensity yielded smaller diabatic peaks [Fig. 1(f)] of *identical* shape, indicating the same relative final-state distribution. A more intense beam that gave
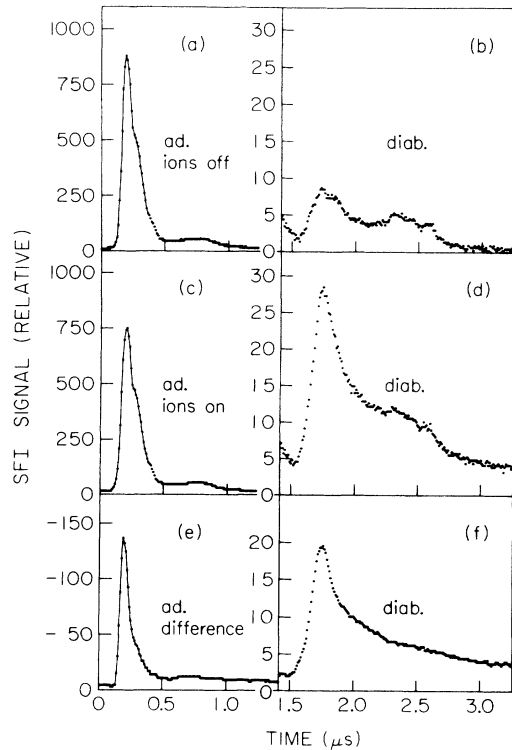
FIG. 1. Adiabatic and diabatic selective field ionization (SFI) following 29-eV Na$^+$ bombardment of Na(28d). Sublevels $|m_l| = 0$, 1, and 2, and hence the entire d state, form the adiabatic SFI peak (a) except for a very small background (b) of unknown origin. Under weak ion bombardment the adiabatic peak (c) is reduced about 8% by transitions into $l \geq 3$ states having sublevels $|m_l| \geq 3$ that undergo SFI diabatically (d). The adiabatic difference signal (e) has an altered shape and consists of partially compensating contributions from d and $l \geq 3$ states. The diabatic difference signal (f) is interpreted as a combination of f,g,h and higher angular momentum states of $n = 28$. The signals (a)–(f) are in the relative proportions indicated by the respective vertical scales.
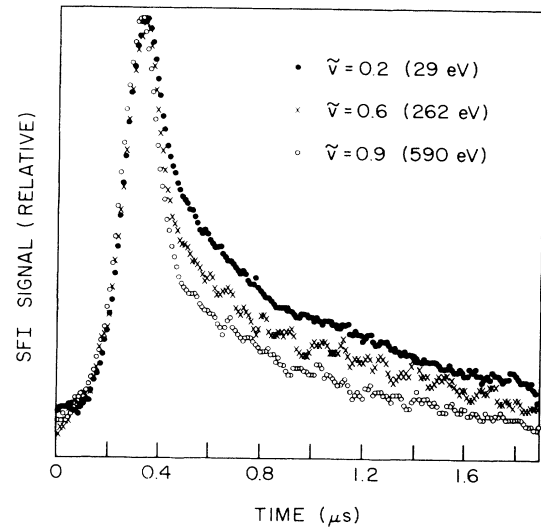

FIG. 2. Selective field ionization from $|m_l| \geq 3$ Stark sublevels of $l \geq 3$ states populated in slow l-change collisions. Electric field slew rate 222.9 V/cm μs. The time origin of this and subsequent figures is shifted by 1.4 μs with respect to that of Fig. 1.

25% adiabatic depopulation produced a broadened diabatic tail indicative of multiple collisions (investigated in detail in Ref. 3). Figure 2 shows the shapes of *weak*-bombardment diabatic signals. A significant broadening is apparent at the lower velocities. This broadening implies increased proportions of higher l states produced by dipole-forbidden transitions and is the subject of the analysis described below.

III. MICROWAVE-RESONANCE DETERMINATION OF f, g, AND h FIELD-IONIZATION PROFILES

For the earlier analysis of multiple collisions,[3] and for a preliminary analysis of the present data,[6] SFI signals were numerically synthesized for selected final-state ensembles from calculated hydrogenic Stark levels and field-ionization rates for $|m_l| \geq 3$ states. They were used as basis functions in a multiparameter least-squares fit of the experimental signals to infer the final-l distribution. However, for the present study the actual SFI sig-

natures of 28f, 28g, and 28h states, under conditions identical to those of the collision experiments, were separately determined by single- and double-quantum microwave resonance.[10,11] In order to drive $\Delta m_j = \pm 1$ resonances from Na(28d) to Na(28f) so that $|m_l| \geq 3$ Stark sublevels would be seen in diabatic SFI, a 1.6-mm-diam stainless-steel rod used as a microwave probe was inserted horizontally between the field plates. Its tip lay 1.3 cm from the mean position of the Rydberg atoms. Microwaves were coupled to the probe through coaxial cable, and the small horizontal component of the oscillating electric field beyond the hemispherical probe tip drove the transitions. The 28d-28f electric dipole resonance (with unresolved fine structure) was excited with 10 μW forward power at 3970 MHz and resulted in a large narrow peak in the SFI spectrum located at the low-field edge of the region where collisional population of $l \geq 3$ states had been observed (Fig. 3). The 28d-28g two-quantum electric dipole resonance, excited with 10 mW from an oscillator at 2163 MHz, yielded a broader SFI peak shifted slightly toward larger fields. The 28d-28h transition, a single-quantum resonance made observable by Stark mixing in small stray electric fields, was driven with 10 mW at 4340 MHz, yielding a broader SFI peak at still higher fields. The center frequencies of observed 28d-28l resonances ($l = 3$, 4, and 5) were close to those predicted on the basis of microwave studies in Na $14 \leq n \leq 16$ (Table I).[10] The three resonance SFI signals were then used as basis functions for a fit of the collisionally produced high-l distributions. In order to improve the fits of the high-field tails of the collision data, the basis was augmented by two numerically synthesized SFI curves corresponding to higher l states of the type used in Ref. 3. The curve marked "18-19" in Fig. 3 used a uniform mixture of Stark levels (n_1,m) that connected

TABLE I. Extrapolated d-f, d-g, and d-h intervals, based on a $A/n^3 + B/n^5$ fit to accurate measurements in $n = 14-16$ (Ref. 10). The fine structure of these transitions is mainly due to the 4.5-MHz $28d$ doublet separation. Applied frequencies at which the resonances were observed are also given.

Interval (MHz)	$28d_{5/2}$-$28f_{7/2}$	$28d_{5/2}$-$28g_{9/2}$	$28d_{5/2}$-$28h_{11/2}$
Extrapolated frequency	3975	4334	4413
Applied frequency	3970	4326 (2×2163)	4340

adiabatically to angular momentum states $l = 18$ and 19 in zero field, with $|m_l| \geq 3$. (The adiabatic connection for Na $l \geq 2$ states is $n_1 = l - |m_l|$, $m = |m_l|$.) Curve "20-23" used similar Stark levels for $l = 20-23$. The role of the two extra basis functions was to prevent the extended tails of the experimental data from "pulling" the inferred $28g$ and $28h$ populations in the fitting procedure. The results were insensitive to the exact curves chosen for this purpose, which were selected to fit the high-field tails smoothly and yield a low χ^2 for the entire fit.

IV. m DEPENDENCES OF THE COLLISIONAL AND MICROWAVE-EXCITED STATES

The $|m_l|$ content of the final-state distributions indicated by Figs. 1 and 2 are not known apart from the fact that some $|m_l| \geq 3$ sublevels are present to yield diabatic SFI. Furthermore, the $|m_l|$ content of the microwave-excited SFI signals of $28f$, g, and h states (Fig. 3) are not known either, and the $|m_l|$ distributions of collisional and microwave-excited states are not
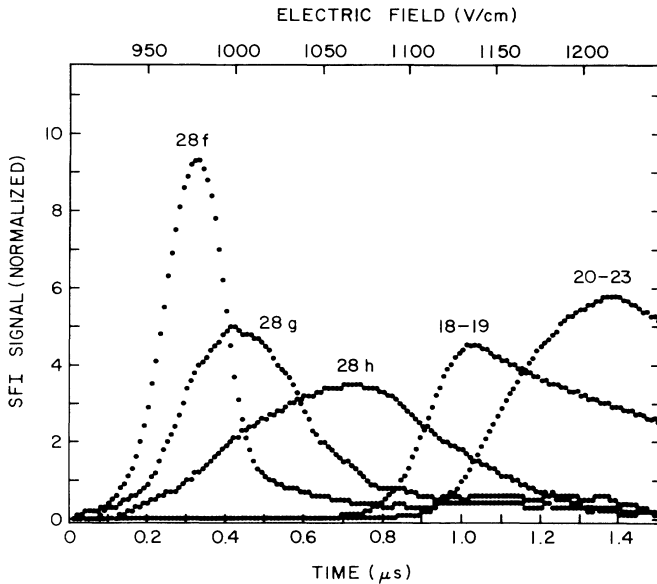
ELECTRIC FIELD (V/cm)

FIG. 3. Diabatic SFI records of microwave-excited $28f$, g, and h states normalized to equal areas. "18-19" and "20-23" are numerically synthesized curves used to augment the basis set.

the same. In this section, reasonable conjectures are developed for the respective distributions, and the sensitivity of the collisional interpretation to various assumptions about the $|m_l|$ distributions is discussed.

A. Collisionally excited states

The collision geometry is cylindrically symmetrical about the horizontal ion-beam axis. An individual ion-Rydberg encounter would have only a lower symmetry, that of reflection in the scattering plane, if the scattered projectile were detected in coincidence with the l-changed Rydberg atom and the orientation of the scattering plane were thus determined. In the present case, however, the density matrix that describes the final-state distribution includes an averaging over azimuths about the ion beam. The density matrix $\rho^{(l)}$ for final states nl is thus diagonal, and its entries, proportional to the cross sections $\sigma(m_l)$ for production of final states m_l, moreover are symmetrical with respect to sign change of m_l. (We ignore electron spin in the following analysis.) Thus, with zeros off the diagonal,

$$\rho^{(l)} = \begin{bmatrix} \sigma(l) & & & & \\ & \sigma(l-1) & & & \\ & & \ddots & & \\ & & & \sigma(l-1) & \\ & & & & \sigma(l) \end{bmatrix} . \quad (2)$$

Detection is carried out by applying a strong electric field perpendicular to the ion-beam axis, and it is with respect to this axis that the $|m_l|$ sublevels are defined for SFI. Transformation of $\rho^{(l)}$ to the detection frame is described by the well-known $d^j_{mm'}(\beta)$ matrices of angular momentum theory[12,13] with $\beta = \pi/2$,

$$\rho^{(l)'}_{m''m'''} = \sum_m d^l_{m''m}(\pi/2)\sigma(m)d^l_{m'''m}(\pi/2) . \quad (3)$$

The values of $d^l_{mm'}(\pi/2)$ involve only summations of algebraic expressions.[12] The resulting $\rho^{(l)'}$ is a symmetric matrix that is diagonal only if $\sigma(m_l)$ is independent of m_l. However, like $\rho^{(l)}$, it is symmetric about the contrary diagonal (interchange of corresponding positive and negative values of m_l). We have calculated $\rho^{(l)'}$ in terms of $\sigma(|m_l|)$ for $l \leq 9$. Figure 4 illustrates a general feature of the results, that the effect of a $\pi/2$ rotation is to distribute the low $|m_l|$ broadly across $|m_l'|$, slightly favoring the highest $|m_l'|$; and high $|m_l|$ is

transformed to $|m_l'| \sim 0$. Diabatic SFI occurs for $|m_l'| \geq 3$. If the sublevel population in the collision frame were presumed uniform for $|m_l| = 0$ to M, and zero beyond, then a fraction F_M of the total population of state nl would be detected by diabatic SFI, where $F_M \rightarrow (2l-4)/(2l+1)$ as $M \rightarrow l$. Figure 5 illustrates the variation of F_M for truncated $|m_l|$ distributions.

Laser excitation of Na(28d) produces target m_j values prior to ion impact that depend on the laser beam directions and polarizations. Excitation through the $3\,{}^2P_{3/2}$ intermediate state populated both fine-structure levels of the 28d state, and thus all values $0 \leq |m_l| \leq 2$ were represented. Nothing is known about the Δm_l behavior of the slow ion-Rydberg l-change process. However, semiclassical arguments that assume a transverse momentum transfer to the active electron suggest that the final angular-momentum vectors would be widely dispersed or uniform in their orientations. The model at the opposite extreme, corresponding to $\Delta m_l = 0$ collisions and $M = 2$, would also yield an approximately uniform distribution in the rotated frame, according to Fig. 4. That the $|m_l'|$ distribution is approximately uniform has been assumed without discussion in our earlier work. The largest relative error in making a "uniform-m" assumption, as compared with an $M = 2$ truncated distribu-
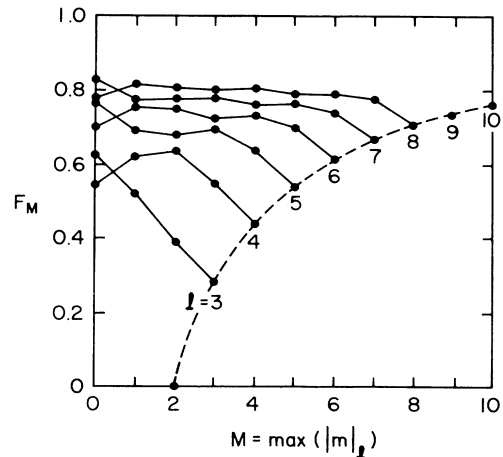
FIG. 5. Fraction F_M of the total population of state nl would be detected by diabatic SFI ($|m_l'| \geq 3$) for truncated uniform distributions $|m_l| \leq M$ in the collision frame. The dashed curve smoothly joins points corresponding to isotropic distributions, $M = l$.

tion occurs for the f state (Fig. 5), but it is for this same final state that the fine-structure precession of l about j, at the fine-structure frequency, approximately (8 MHz)/$l(l+1) = 0.7$ MHz, is most rapid and the m_l' values thus most thoroughly blended.

B. Microwave-excited states

The $|m_l'|$ values represented by the microwave-induced SFI curves depend upon laser polarizations as before and upon the direction of the oscillating electric field produced by the microwave probe. The oscillating field is approximately horizontal, although for noncentrally located Rydberg atoms the field may have a small vertical component. The single-quantum microwave transitions are thus dominated by $\Delta m_j = \pm 1$ relative to the SFI field direction. In general, all $|m_l'|$ components will be present in the microwave-excited states, but the exact proportions depend on fine-structure coherences produced by the pulsed laser and the characteristics of the passage from low fields (where the good quantum numbers are $lsjm_j$) to intermediate fields (where good quantum numbers are lsm_lm_s).[14]

In order to assess the sensitivity of field-ionization signals to $|m_l'|$, we synthesized SFI curves for the Stark levels that evolve adiabatically from the various l, m_l intermediate-field states and ionize in an electric-field ramp whose slew rate was that used in the experiments ($dF/dt = 222.9$ V/cm μs). Each individual Stark level yielded a slightly skewed bell-shaped peak. Centers and widths are listed in Table II. There it can be seen that the dependence of peak positions on m_l for $l \leq 16$ is much smaller than the width of a single peak, amounting to only 5 to 12 V/cm per $\Delta m = 1$ step. In contrast the microwave-excited 28g peak (Fig. 3) is offset 27 V/cm from 28f, and the 28h is offset 54 V/cm from 28g. The SFI peak positions would thus be little affected by changing the balance of their constituent $|m_l| = 3$, 4, and 5 sublevels.
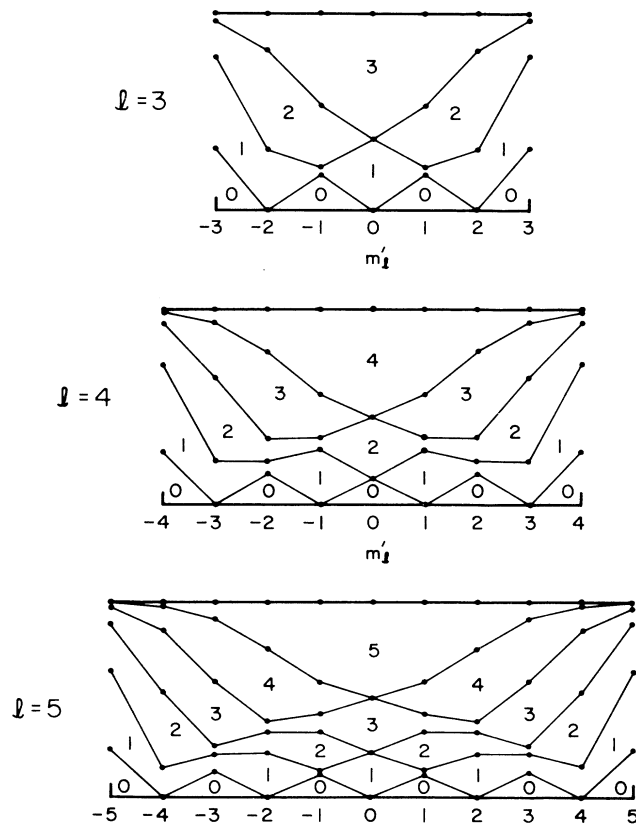

FIG. 4. Distribution of m_l' sublevels in the rotated (detector) frame based on truncated uniform collision-frame distributions that are defined by max($|m_l|$) = M. The region indicated by, e.g., $M = 3$ is derived from unrotated $m_l = \pm 3$ sublevels. $M = l$ defines a uniform distribution in both frames.

TABLE II. Centers at half maximum for numerically synthesized SFI signals from $n=28$ Stark levels. Each curve has full width at half maximum 25 V/cm and is skewed somewhat toward high fields. Slew rate $dF/dt=222.9$ V/cm μs.

l	m_l	n_1	Center (V/cm)	l	m_l	n_1	Center (V/cm)
3	3	0	966	12	3	9	1080
4	3	1	975	12	4	8	1075
4	4	0	971	12	5	7	1068
5	3	2	985	14	3	11	1125
5	4	1	980	14	4	10	1114
5	5	0	976	14	5	9	1105
6	3	3	996	16	3	13	1173
6	4	2	990	16	4	12	1161
6	5	1	985	16	5	11	1150
8	3	5	1020	18	3	15	1204
8	4	4	1015	18	4	14	1216
8	5	3	1009	18	5	13	1204
10	3	7	1050	20	3	17	1304
10	4	6	1043	20	4	16	1286
10	5	5	1035	20	5	15	1269

The centers and widths of the microwave-excited peaks (Fig. 3) do not agree with corresponding values from Table II. In fact, the $28f$ peak would agree better with a superposition of $|m_l|=3$ sublevels of $l=3$, 4, and 5 states, the $28g$ with $|m_l|=3$ and 4 of $l=4-10$, and the $28h$ with $|m_l|=3$ of $l=5-14$. (The suggested ranges of l and $|m_l|$ reflect the electric dipole selection rules for the corresponding microwave transitions and include l's from the nominal value upward.) The disagreement of SFI peaks may indicate an effect that is different from the uncertainty of m values, namely that during the early part of the electric-field ramp, probably during the first 1 V/cm, the evolution from uncoupled angular momentum state (l,m_l) to Stark state (n_1,m) may be nonadiabatic. If the logarithmic derivative with respect to time of the energy difference between two diverging Stark levels is not small compared with the Bohr frequency of the corresponding transition, then the adiabaticity condition for the state evolution is not satisfied,[15] and n_1 mixing may occur. The same mixing would occur following microwave excitation of an l state as would occur after collisional excitation of the same state. The use of identical SFI ramp profiles in the two

phases of the present study validates the SFI curves for $28f$, $28g$, and $28h$ for our apparatus. The experimental and theoretical study of nonadiabatic mixing in the ramp is left to future work.

Thus the indefiniteness of the $|m_l|$ distributions both in the collisional and microwave-excited population, under reasonable assumptions, has little influence on the inferred final-l distributions.

In one respect the conditions of microwave and collisional excitation and detection differed: It may be significant that the microwaves remained on during the SFI electric-field ramp. Pulsing the microwaves off in the case of the $28d$-$28f$ resonance did not change the corresponding SFI signal, and we expect the same for the other resonances. However, in future work the microwaves must be pulsed on only during the interval between the laser flash and the beginning of the ramp.

V. FITTING RESULTS: INFERRED l DISTRIBUTIONS

The results of the five-parameter fits of the diabatic peaks for collisions at eight energies from 29 to 590 eV

TABLE III. Fractional populations of Na($28l$) states after l change from Na$^+$ impact on Na($28d$) at energy E. The final-state distribution is inferred from a fit of the diabatic selective field-ionization signals using as model functions the $n=28$ f, g, and h states populated by microwave resonance and numerically synthesized signals for $l>5$ (Fig. 3). Each collisionally populated l state was assumed to have a uniform distribution among m_l sublevels (see text).

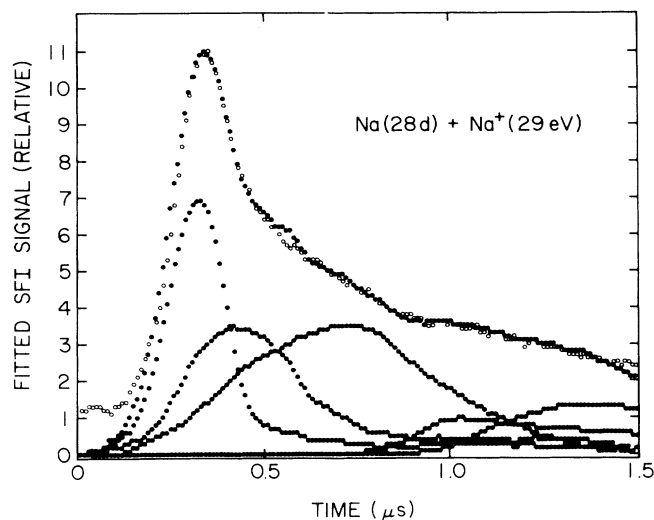| E (eV)	v	$l=3$	$l=4$	$l=5$	$l>5$
29	0.2	0.373	0.227	0.265	0.135
65	0.3	0.420	0.190	0.262	0.128
117	0.4	0.438	0.189	0.243	0.130
182	0.5	0.419	0.198	0.248	0.135
262	0.6	0.460	0.184	0.234	0.122
360	0.7	0.505	0.179	0.221	0.096
465	0.8	0.533	0.157	0.212	0.099
590	0.9	0.588	0.120	0.212	0.081

FIG. 6. Least-squares fit to the 29-eV diabatic SFI collision data (open circles), showing the component curves (Fig. 3) and their sum (solid dots).

FIG. 7. Cumulative fractional final-l distributions in $Na^+ + Na(28d)$ collisions for assumed final-m distributions $\max(\,|\,m_l\,|\,) \equiv M = 0$, 2, and l (see text). Dashed lines: coupled-channel calculations, Ref. 4.

are listed in Table III. It was assumed in the analysis that all m sublevels of a given l were equally populated, but the results of Figs. 4 and 5 can be applied to convert the results to truncated m distributions defined by $\max(\,|\,m_l\,|\,) = M$. The typical quality of the fits is illustrated in Fig. 6. The final-state distribution coefficients are shown in a cumulative form in Fig. 7. The three shaded bands mark the extremes of inferred l distributions in the collision frame corresponding to $M=0$ and $M = l$. There is little difference between $M = 2$ and l, and the latter (i.e., the all-m case) is recommended. The results show a substantial, and velocity-dependent, degree of dipole-forbidden behavior for $\bar{v} \leq 0.9$. Below $\bar{v} = 0.7$ more than half of final states are dipole forbidden from $28d$. The agreement with the coupled-channel calculations[4] for $\bar{v} \geq 0.7$ is satisfactory, although the calculations predict more $28g$ and less $28h$ than experimentally observed in that range. (This difference could reflect a shortcoming in the experimental analysis based upon the microwave-excited SFI results of Fig. 3.) However, although the trend for $\bar{v} < 0.7$ toward greater population of $l > 3$ at the expense of the f state is clearly shown by the
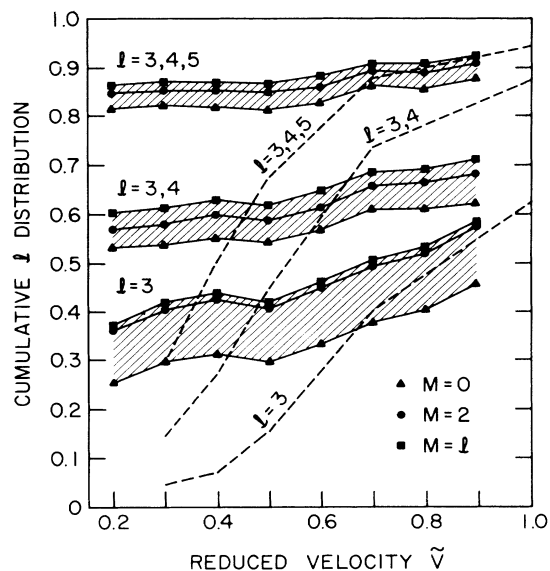
data, more than 85% of final states $28l$ are accounted for by $l = 3$, 4, and 5 at all velocities measured. The coupled-channel calculations predict that only 30% of final states have $l = 3$, 4, and 5 at $v = 0.3$.

In conclusion, l change in slow $Na^+ + Na(28d)$ collisions populates $l > 3$ states through dipole-forbidden transitions under single-collision conditions despite the validity of the dipole approximation for the perturbing potential. The degree of this strong-coupling behavior increases as the projectile velocity is decreased, in qualitative although not quantitative agreement with the coupled-channel calculations of Beigman and Syrkin.

ACKNOWLEDGMENTS

[1]K. B. MacAdam, R. G. Rolfes, and D. A. Crosby, Phys. Rev. A **24**, 1286 (1981).

[2]I. C. Percival, in *Atoms in Astrophysics*, edited by P. G. Burke, W. B. Eissner, D. G. Hummer, and I. C. Percival (Plenum, New York, 1983), p. 75.

[3]K. B. MacAdam, D. B. Smith, and R. G. Rolfes, J. Phys. B **18**, 441 (1985).

[4]I. L. Beigman and M. I. Syrkin, Zh. Eksp. Teor. Fiz. **89**, 400 (1985) [Sov. Phys.—JETP **62**, 226 (1985)].

[5]W. W. Smith, P. Pillet, R. Kachru, N. H. Tran, and T. F. Gallagher, *Abstracts of Contributed Papers, 13th International-*

al Conference on the Physics of Electronic and Atomic Collisions, Berlin, edited by J. Eichler et al. (North-Holland, Amsterdam, 1983), p. 668.

[6]K. B. MacAdam, R. G. Rolfes, X. Sun, and D. B. Smith, Nucl. Instrum. Methods B **24/25**, 280 (1987). The present collision data were discussed briefly in this conference proceeding, but the microwave measurements and subsequent analysis post-date that work. The discrepancy between the 56% $l \leq 5$ with Ar^+ impact at $\bar{v} = 0.89$ cited above and in Ref. 3 and the present result, 92% $l \leq 5$ at $\bar{v} = 0.9$ (Table III), is attributable to the different sets of curves used

to model the f, g, and h states. The analysis given in Ref. 6, based entirely on numerically synthesized f, g, and h curves, gives 51% $l \leq 5$ at $\bar{v}=0.9$, which is consistent with Ref. 3.

[7]F. G. Kellert, T. H. Jeys, G. B. McMillian, K. A. Smith, F. B. Dunning, and R. F. Stebbings, Phys. Rev. A **23**, 1127 (1981).

[8]W. L. Fuqua III and K. B. MacAdam, Rev. Sci. Instrum. **56**, 385 (1985).

[9]T. H. Jeys, G. W. Foltz, K. A. Smith, E. J. Beiting, F. G. Kellert, F. B. Dunning, and R. F. Stebbings, Phys. Rev. Lett. **44**, 390 (1980).

[10]T. F. Gallagher, R. M. Hill, and S. A. Edelstein, Phys. Rev. A **14**, 744 (1976).

[11]K. B. MacAdam and W. H. Wing, Phys. Rev. A **15**, 678 (1977).

[12]D. M. Brink and G. R. Satchler, *Angular Momentum* (Oxford University Press, New York, 1968).

[13]A. R. Edmonds, *Angular Momentum in Quantum Mechanics* (Princeton University Press, Princeton, N.J., 1960).

[14]T. H. Jeys, G. B. McMillian, K. A. Smith, F. B. Dunning, and R. F. Stebbings, Phys. Rev. A **26**, 335 (1982).

[15]L. I. Schiff, *Quantum Mechanics*, 3rd ed. (McGraw-Hill, New York, 1968).